催化学报
2012 Chinese Journal of Catalysis Vol. 33 No. 1

文章编号: 0253-9837(2012)01-0174-09 国际版 DOI: 10.1016/S1872-2067(11)60325-2 研究论文: 174~182

二乙胺导向合成SAPO-34及与其它模板剂的对比

刘广宇[1,2], 田 鹏[1], 刘中民[1,*]

[1]中国科学院大连化学物理研究所, 辽宁大连 116023

[2]河南工业大学化学化工学院, 河南郑州 450001

摘要: 以二乙胺(DEA)为模板剂, 合成了SAPO-34分子筛, 详细考察了磷酸用量、水用量以及硅源和铝源等因素的影响. 结果表明, 在 $0.7 \le n(P_2O_5)/n(Al_2O_3) \le 1.2$ 及 $25 \le n(H_2O)/n(Al_2O_3) \le 100$ 范围内, 可以得到纯相SAPO-34分子筛, 铝源对所得样品的组成影响较大. 同时, 采用三乙胺(TEA)、吗啉(MOR)以及二乙胺-三乙胺(DEA-TEA)混合模板剂合成了SAPO-34, 通过X射线衍射、X射线荧光分析、扫描电镜、热重和^{29}Si固体核磁共振等手段对所得样品进行了表征. 结果显示, 不同模板剂促使硅进入SAPO-34骨架的能力顺序为SAPO-34 (DEA) > SAPO-34 (MOR) > SAPO-34 (TEA); SAPO-34骨架中所能容纳的最大Si(4Al)含量顺序为SAPO-34 (DEA) ≈ SAPO-34 (MOR) > SAPO-34 (TEA).

关键词: SAPO-34; 模板剂; 二乙胺; 三乙胺; 吗啉; 合成

中图分类号: O643 **文献标识码**: A

收稿日期: 2011-09-03. 接受日期: 2011-10-21.

*通讯联系人. 电话/传真: (0411)84685510; 电子信箱: liuzm@dicp.ac.cn

本文的英文电子版(国际版)由Elsevier出版社在ScienceDirect上出版(http://www.sciencedirect.com/science/journal/18722067).

Synthesis of SAPO-34 Molecular Sieves Templated with Diethylamine and Comparison with Other Templates

LIU Guangyu[1,2], TIAN Peng[1], LIU Zhongmin[1,*]

[1]*Dalian Institute of Chemical Physics, Chinese Academy of Sciences, Dalian 116023, Liaoning, China*

[2]*School of Chemistry & Chemical Engineering, Henan University of Technology, Zhengzhou 450001, Henan, China*

Abstract: SAPO-34 molecular sieves were synthesized using diethylamine (DEA) as a template. Influencing factors, such as H_3PO_4 content, H_2O content, Al source, and Si source, were investigated. Pure SAPO-34 could be obtained under the following synthesis gel conditions: $0.7 \le n(P_2O_5)/n(Al_2O_3) \le 1.2$ and $25 \le n(H_2O)/n(Al_2O_3) \le 100$. The Al source has a great influence on the resulting sample composition. SAPO-34 could also be synthesized using triethylamine (TEA), morpholine (MOR), and a DEA-TEA mixture as template, respectively. The products were characterized using X-ray diffraction, X-ray fluorescence, scanning electron microscopy, thermogravimetry, and ^{29}Si MAS NMR. The level of silicon incorporation into the SAPO-34 framework decreased in the following order of SAPO-34 (DEA) > SAPO-34 (MOR) > SAPO-34 (TEA). The Si(4Al) contents in the SAPO-34 frameworks followed the order of SAPO-34 (DEA) ≈ SAPO-34 (MOR) > SAPO-34 (TEA).

Key words: SAPO-34; template; diethylamine; triethylamine; morpholine; synthesis

Received 3 September 2011. Accepted 21 October 2011.

**Corresponding author. Tel/Fax: +86-411-84685510; E-mail: liuzm@dicp.ac.cn*

English edition available online at Elsevier ScienceDirect (http://www.sciencedirect.com/science/journal/18722067).

SAPO-34分子筛具有适宜的孔道结构、合适的酸性及高水热稳定性, 因而在甲醇制烯烃反应(MTO)中表现出优良的低碳烯烃选择性, 被认为是理想的MTO催化剂[1~6], 具有重要的工业应用价值.

合成SAPO-34分子筛可采用多种模板剂, 如四乙基氢氧化铵[6~8]、异丙胺[7]、二丙胺[7]、哌啶[9]、吗啉(MOR)[7,10]、三乙胺(TEA)[11~13]、二乙胺(DEA)[14~16]等以及它们的混合物. 一般认为, 模板剂

在分子筛合成过程中起结构导向、电荷匹配和空间填充作用[17]. 模板剂的种类对合成的分子筛结构和物化性质等的影响很大. 目前人们对此进行了研究[18~21], 但研究主要集中在模板剂对所得SAPO-34晶粒大小及催化性能的影响. 而有关模板剂对分子筛酸性质影响的本质原因, 即硅进入分子筛骨架的程度及分布状况等并未进行细致研究.

近期我们以DEA为模板剂, 合成了SAPO-34分子筛, 并考察了其催化MTO反应的性能[15]. 本文详细考察了该合成过程各因素的影响, 以获得优化的合成条件; 同时, 比较了DEA, TEA和MOR等常用的几种有机胺为模板剂合成样品的特点, 以深入理解SAPO-34的合成过程.

1 实验部分

1.1 分子筛的合成

采用水热晶化法合成SAPO-34分子筛. 将铝源、硅源(除特别说明外, 分别为拟薄水铝石、硅溶胶)、磷酸与去离子水混合, 室温搅拌1 h后加入模板剂, 继续搅拌至形成均匀的凝胶, 再移入200 ml的聚四氟乙烯内衬的不锈钢合成釜中, 密闭加热到200 ºC, 在自身压力下晶化24 h. 典型凝胶摩尔比为2.0DEA:0.6SiO_2:1.0Al_2O_3:0.8P_2O_5:50H_2O. 待晶化完全后将固体产物离心分离, 并用去离子水洗涤至中性, 在120 ºC空气中干燥后, 得到SAPO-34分子筛原粉. 原粉在550 ºC空气中焙烧5 h除去有机模板剂后即为焙烧型样品.

1.2 分子筛的表征

分子筛样品的X射线衍射(XRD)测试在日本理学的D/max-γb型X射线衍射仪上进行, Cu靶, K_α辐射源(λ = 0.15406 nm), 电压40 kV, 电流40 mA. 样品形貌由KYKY-AMRAY-1000B型扫描电子显微镜(SEM)观测. 样品组成采用Philips公司的Magix 2424 X射线荧光分析(XRF)仪测定.

热分析在美国Perkin-Elmer公司的Pyris-1 TGA型热分析仪上进行, 空气气氛, 升温速率10 ºC/min.

^{29}Si固体核磁共振(^{29}Si MAS NMR)谱在Varian Infinity-plus 400 WB型固体核磁共振波谱仪上测量, 使用BBO MAS探头和7 mm ZrO_2样品管, 共振频率为79.5 MHz, 转速为4 kHz, 化学位移以三甲基硅丙磺酸钠(DSS)为参考外标.

2 结果与讨论

2.1 DEA合成SAPO-34的影响因素

2.1.1 磷酸用量

固定合成原料摩尔配比为2.0DEA:0.6SiO_2:1.0Al_2O_3:$n$$P_2O_5$:50$H_2O$, 考察了$H_3PO_4$(即$P_2O_5$)用量对SAPO-34合成的影响, 所得样品的XRD谱见图1. 可以看出, 随初始凝胶中P_2O_5用量增加, 晶化前后pH值均呈下降趋势. 当n(P_2O_5)为0.5时, 产物为无定形的一水软铝石胶; 至0.6时开始有SAPO-34生成; 在n(P_2O_5)为0.7~1.2时可得到纯的SAPO-34; 继续增大P_2O_5用量, 产物中开始出现具有十元环孔道的AFO型SAPO-41分子筛; 当n(P_2O_5)为1.5时, 产物中已经没有SAPO-34.

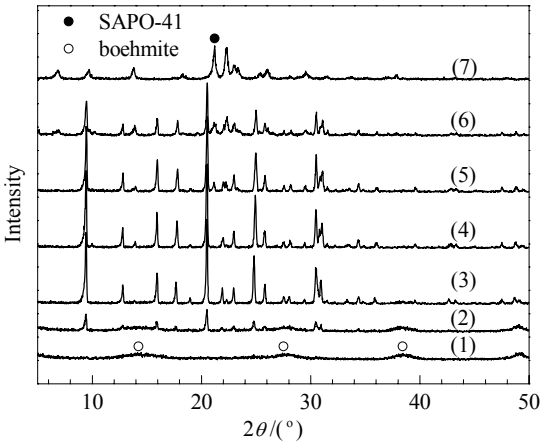

图 1 不同H_3PO_4用量合成样品的XRD谱

Fig. 1. XRD patterns for samples synthesized with different H_3PO_4 amounts in the initial gel (2.0DEA:0.6 SiO_2:1.0Al_2O_3:$n$$P_2O_5$:50$H_2O$). n(P_2O_5) = (1) 0.5; (2) 0.6; (3) 0.7; (4) 1.2; (5) 1.3; (6) 1.4; (7) 1.5.

2.1.2 水用量

固定合成原料摩尔配比为2.0DEA:0.6SiO_2:1.0Al_2O_3:0.8P_2O_5:$n$$H_2O$, 考察了$H_2O$用量对SAPO-34合成的影响, 结果见表1. XRD结果表明, 当H_2O量为15~300时均可得到SAPO-34. 由表可见, 晶化前合成凝胶的pH值基本相同, 约为6.0, 晶化后凝胶pH值随H_2O量的增加而降低. SAPO-34收率在n(H_2O) > 25时随水量增多而下降. 当n(H_2O) < 50, 样品相对结晶度随H_2O量增多而增大, 至50时达最大; 当水量超过50, 样品结晶度降低, 至300时降到33%, 有一些无定形铝物种生成.

化学元素分析显示, 合成样品中硅含量随H_2O

表 1 H_2O 用量对 SAPO-34 合成的影响

Table 1 Effect of H_2O content in the initial gel on the synthesis of SAPO-34

$n(H_2O)$	pH before crystallization	pH after crystallization	Relative crystallinity (%)	Relative yield (%)	Molar composition
15	5.5	9.0	88	48	$Si_{0.169}Al_{0.496}P_{0.335}O_2$
25	6.0	9.0	93	100	$Si_{0.154}Al_{0.494}P_{0.352}O_2$
50	6.0	8.0	100	79	$Si_{0.150}Al_{0.494}P_{0.356}O_2$
100	6.0	8.0	78	71	$Si_{0.131}Al_{0.571}P_{0.299}O_2$
300	6.0	6.0	33	44	$Si_{0.096}Al_{0.697}P_{0.207}O_2$

量增多而下降. H_2O 量过少时, 晶化体系的液相离子浓度高, 合成的推动力大, 随着晶化产物的生成, 体系 pH 值升高, 从而导致合成产物的溶解度增加, 使得产率下降. 我们前期的研究[15]也发现, 增大 DEA 用量 (pH 值升高), 产物中硅含量增加, 但产率降低. H_2O 量过多时, 晶化体系的液相离子浓度较低, 合成的推动力变小, 晶化产率降低. 因此, $n(H_2O)$ 为 25~100 比较适宜.

2.1.3 硅源和铝源

固定合成凝胶摩尔配比, 考察了不同反应活性和聚合度的硅源 (硅溶胶、白碳黑、正硅酸乙酯) 及铝源 (拟薄水铝石、异丙醇铝、氯化铝、铝溶胶) 对 SAPO-34 的影响, 结果见表 2. 可以看出, 除了以合成铝溶胶为铝源、硅溶胶为硅源时, 所得样品不是 SAPO-34 外, 其余的样品均为结晶度很高的 SAPO-34 分子筛纯相. 这是因为 SAPO 分子筛的合成需要弱酸性或中性条件, 而以铝溶胶为铝源时所制凝胶 pH 值较低 (0.5), 酸性较强 (凝胶制备过程没有另外调节 pH 值), 使合成凝胶变为 α-石英相.

表 2 铝源及硅源对 SAPO-34 合成的影响

Table 2 Effects of the Al source and Si source on the synthesis of SAPO-34 products

Silica source	Alumina source	Product	Relative crystallinity (%)	Molar composition
Fume silica	pseudoboehmite	SAPO-34	108	$Si_{0.157}Al_{0.501}P_{0.342}O_2$
$Si(OC_2H_5)_4$	pseudoboehmite	SAPO-34	94	$Si_{0.157}Al_{0.514}P_{0.329}O_2$
Silica sol	pseudoboehmite	SAPO-34	100	$Si_{0.150}Al_{0.494}P_{0.356}O_2$
Silica sol	$Al(i\text{-}OC_3H_7)_3$	SAPO-34	87	$Si_{0.093}Al_{0.527}P_{0.380}O_2$
Silica sol	$AlCl_3$	SAPO-34	90	$Si_{0.106}Al_{0.498}P_{0.396}O_2$
Silica sol	alumina sol	α-quartz	—	—

由表 2 可见, 铝源对合成样品的组成影响较大. 以硅溶胶为硅源, 其中以异丙醇铝为铝源时所得样品的硅含量最低, 以拟薄水铝石为铝源时最高. 这可能是因为单体铝源异丙醇铝的活性较高, 与磷酸反应的活性要高于聚合态的铝源, 如拟薄水铝石. 异丙醇铝与磷酸混合后, 可以很快形成磷酸铝前驱体. 硅溶胶为聚合态的硅源, 其解聚释放出活性硅物种的速率可能相对较慢, 抑制了硅取代骨架 P 或 P-Al 对的过程, 从而导致分子筛样品的硅含量相对较低. 另外, 以白碳黑和正硅酸乙酯为硅源合成的样品中硅含量略高于硅溶胶的.

图 2 为不同硅源和铝源合成的 SAPO-34 样品的 SEM 照片. 可以看出, 所得 SAPO-34 样品皆为菱形晶体, 其中以白碳黑或正硅酸乙酯为硅源时所得样品尺寸明显要小于硅溶胶的.

2.2 不同模板剂合成对比研究

本文比较了 DEA, TEA, MOR 以及 DEA-TEA 混合模板剂所得样品的物化性质, 具体合成原料配比

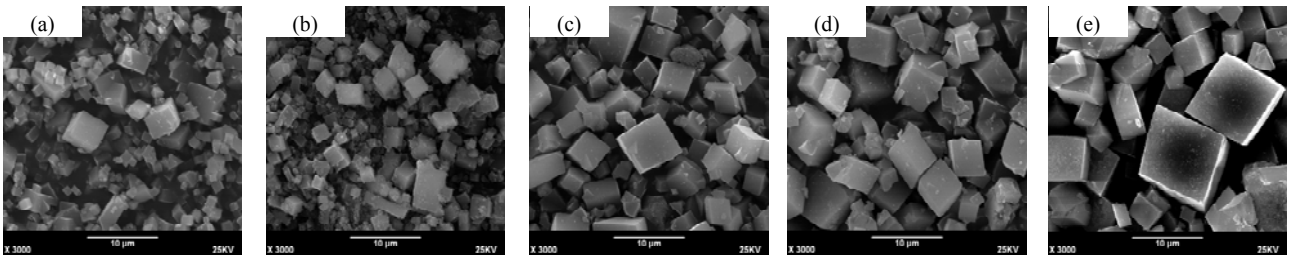

图 2 不同铝源、硅源合成样品的 SEM 照片

Fig. 2. SEM images for samples synthesized with different Al and Si sources. (a) pseudoboehmite and fume silica; (b) pseudoboehmite and $Si(OC_2H_5)_4$; (c) pseudoboehmite and silica sol; (d) $Al(i\text{-}OC_3H_7)_3$ and silica sol; (e) $AlCl_3$ and silica sol.

表 3 不同模板剂合成 SAPO-34 的原料配比及晶化条件

Table 3 Composition of synthesis gels and crystallization conditions for samples synthesized using different templates

Sample	Gel composition					Time (h)	t/°C
	Template	SiO_2	Al_2O_3	P_2O_5	H_2O		
T-0.6Si	2TEA	0.6	1.0	0.8	50	24	200
DT-0.6Si	1DEA+1TEA	0.6	1.0	0.8	50	24	200
D-0.6Si	2DEA	0.6	1.0	0.8	50	24	200
M-0.6Si	2MOR	0.6	1.0	0.8	50	24	200
D-0.4Si	2DEA	0.4	1.0	0.8	50	24	200

和晶化条件见表3.

2.2.1 晶相和元素组成

图3为不同模板剂合成样品的XRD谱. 可以看出, 各样品的衍射峰均与SAPO-34的一致, 其中以TEA为模板剂合成样品(T-0.6Si)的相对结晶度较低, 其余均较高(见表4). 值得注意的是, T-0.6Si样品中几个主峰强度很高, 但高角度部分的衍射峰很弱或缺失. 这有可能是模板剂变化引起的晶体骨架扭曲所致, 也有可能是形成了SAPO-34和SAPO-18的共晶体(含微量的SAPO-18).

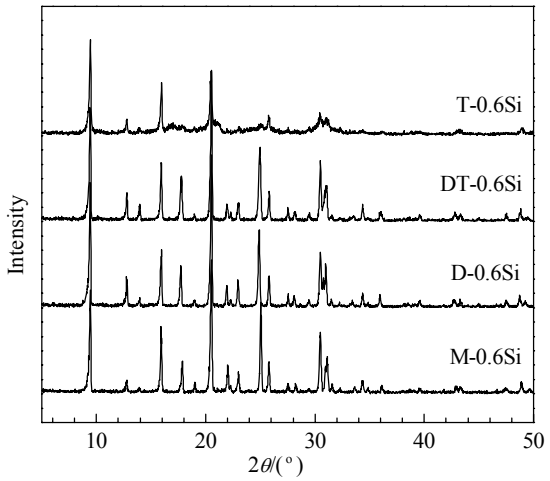

图 3 不同模板剂合成样品的 XRD 谱

Fig. 3. XRD patterns for samples synthesized using different templates.

表 4 SAPO-34 样品的相对结晶度和元素分析结果

Table 4 Relative crystallinity and chemical composition of SAPO-34

Sample	Relative crystallinity (%)	Product composition	Si incorporation*
T-0.6Si	63	$Si_{0.102}Al_{0.484}P_{0.414}O_2$	0.71
DT-0.6Si	97	$Si_{0.128}Al_{0.480}P_{0.392}O_2$	0.90
D-0.6Si	100	$Si_{0.150}Al_{0.494}P_{0.356}O_2$	1.05
M-0.6Si	91	$Si_{0.134}Al_{0.475}P_{0.391}O_2$	0.94
D-0.4Si	—	$Si_{0.134}Al_{0.495}P_{0.371}O_2$	1.34

*Molar ratio of $(Si/(Si + Al + P))_{product}/(Si/(Si + Al + P))_{gel}$.

合成样品的元素分析结果见表4. 可以发现, 单一模板剂合成样品中, DEA合成的SAPO-34骨架中硅含量最高, n(Si)/n(Si + Al + P)为0.150, MOR合成的次之, TEA合成的最低, 为0.102, 可见, 以DEA为模板剂合成样品具有高硅进入的特点. 以DEA-TEA混合模板剂合成的SAPO-34骨架硅含量约等于两者单独合成样品的骨架硅含量平均值, 显示出混合模板剂的“加和”效应.

2.2.2 晶体形貌

图4为合成样品的SEM照片. 可以看出, 以MOR为模板剂合成的SAPO-34样品晶粒最大, 达到10 μm; TEA的最小, 约为2 μm; DEA合成样品D-0.6Si粒径在2~4 μm之间, 而以DEA-TEA混合模板剂合成样品粒径介于DEA和TEA单独合成样品粒径之间.

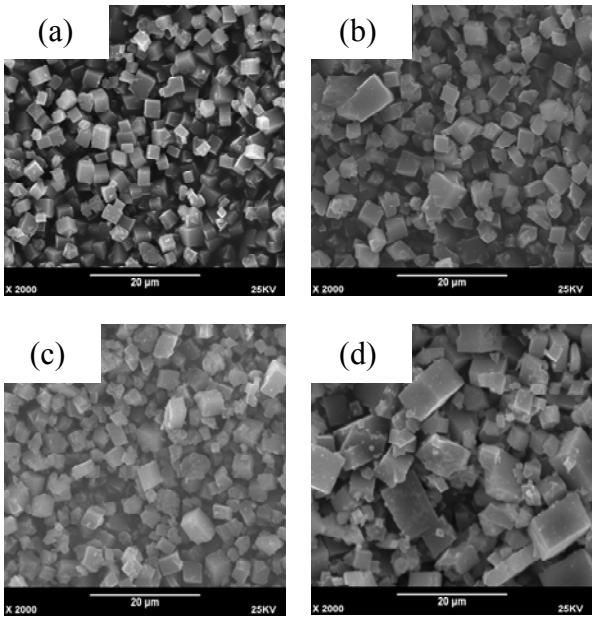

图 4 不同模板剂合成样品的 SEM 照片

Fig. 4. SEM images for samples synthesized using different templates. (a) T-0.6Si; (b) DT-0.6Si; (c) D-0.6Si; (d) M-0.6Si.

2.2.3 热分析

不同模板剂合成的样品在空气气氛下的TG结果显示, 所有样品的失重分为三个阶段, 分别为<200, 200~490和>490 °C. 第一阶段是分子筛上水的脱除; 第二和第三阶段分别对应于分子筛中模板剂的燃烧分解和残留的高碳氢比的有机物的燃烧分解. 表5给出了各阶段的失重结果. 可以看出, 水的

表 5 SAPO-34 的热分析结果

Table 5 Thermal analysis results of SAPO-34

Sample	Percentage of H_2O (%)	Percentage of template (%)	Percentage of template (%)		Moles of template per cage*
			200–490 ºC	> 490 ºC	
T-0.6Si	4.01	11.83	79	21	1.02
DT-0.6Si	3.74	13.06	73	27	1.32
D-0.6Si	4.41	13.96	72	28	1.71
M-0.6Si	4.74	16.53	52	48	1.76

*The molecular weights for the mixed templates are calculated by averaging those for the individual components.

失重比较接近, 而模板剂的失重相差较大: TEA 最小, 为 11.83%; MOR 最大, 为 16.53%. 由 TG 结果可算得分子筛每个 CHA 笼中的平均模板剂数: MOR 最高为 1.76, 与 Prakash 等[22]结果相近; DEA 为 1.71, 接近 MOR; TEA 最低, 为 1.02. 使用 DEA-TEA 混合模板剂, 进入分子筛内的模板剂数量较纯 TEA 有较大增加. 我们认为, 不同模板剂在 CHA 笼中数量的差异主要源自它们分子体积的不同, TEA 由于含有三个乙基支链, 分子体积明显大于只有两个乙基支链的 DEA 和成环状的 MOR.

在分子筛合成中, 模板剂除了结构导向和空间填充作用外, 还具有平衡分子筛骨架电荷的作用. 模板剂所能提供的正电荷数决定了分子筛的骨架负电荷数, 而这些负电荷是由于硅原子进入骨架取代 P 原子或 P-Al 对形成硅岛造成的, 因此模板剂数量也在一定程度上决定了骨架中硅含量. TEA 进入分子筛内的量最少, 所以相应的 SAPO-34 样品中骨架硅含量最低. DEA 进入分子筛内的量与 MOR 接近, 但合成样品中骨架硅含量却比 MOR 高. 这可能是因为分子筛孔笼内的 MOR 有一部分只起孔道填充作用, 并没有起到电荷补偿作用.

2.2.4 ^{29}Si MAS NMR 分析

^{29}Si MAS NMR 可以用来表征 Si 在 SAPO-34 分子筛骨架上的分布状态. 图 5 给出了各样品的 ^{29}Si MAS NMR 谱. 可以看出, 几个样品均在 δ = –92.5, –96.5, –101, –105 和–111 处出现共振峰, 可分别归属为 Si(4Al), Si(3Al), Si(2Al), Si(1Al) 和 Si(0Al) 环境[11,17]. 将各样品谱峰进行高斯拟合, 结果见表 6. 对比 D-0.4Si 和 D-0.6Si 样品, 随着骨架硅含量的增加, 骨架中 Si(4Al) 环境所占比例降低, 相应于硅岛形成的其它硅环境比例增加. 0.6Si 系列样品中, T-0.6Si 和 M-0.6Si 分别具有最低和最高的 Si(4Al) 含量.

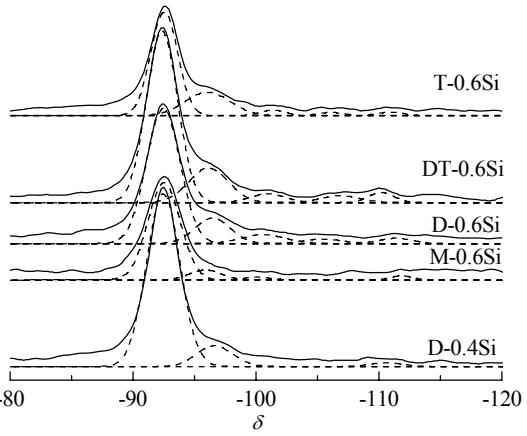

图 5 不同模板剂合成样品的 ^{29}Si MAS NMR 谱

Fig. 5. ^{29}Si MAS NMR spectra of samples synthesized using different templates.

表 6 从 ^{29}Si MAS NMR 谱拟合得到的硅环境分布

Table 6 Distribution of silicon environments observed in the deconvoluted ^{29}Si MAS NMR spectra

Sample	Silicon environments distribution (%)				
	Si(4Al)	Si(3Al)	Si(2Al)	Si(1Al)	Si(0Al)
T-0.6Si	66.80	25.26	3.45	2.09	2.40
DT-0.6Si	71.09	18.08	3.98	3.50	3.36
D-0.6Si	73.75	14.47	6.21	2.80	2.77
M-0.6Si	86.60	8.62	2.09	0.20	2.49
D-0.4Si	87.00	11.20	0.00	0.00	1.80

M-0.6Si 中硅环境分布与 D-0.4Si 的接近. DEA-TEA 混合模板剂样品 DT-0.6Si 的硅环境分布则为两模板剂样品的中间值.

根据拟合所得不同硅环境的比例, 结合表 4, 可算得每个样品的骨架净电荷及相应每个笼中起平衡骨架电荷作用的模板剂数量 A_1; 结合表 5 中 SAPO-34 每个笼中的模板剂分子数, 可算得孔笼中没有起到平衡骨架电荷作用的模板剂数量 A_2, 结果见表 7. 对比具有不同硅含量的 D-0.4Si 和 D-0.6Si, 尽管分子筛孔笼内的模板剂数量相当, 但随着骨架中硅含量的增加, 用于平衡骨架电荷的模板剂数量也增大. 0.6Si 系列样品中, 以 TEA 和 DEA-TEA 为模板剂的 T-0.6Si 和 DT-0.6Si 样品的 A_2 均为 0, 说明这两个样品孔笼中的模板剂全部用于平衡骨架电荷. 以 DEA 和 MOR 为模板剂的样品中, A_2 分别为 0.12 和 0.25, 相应于平衡骨架电荷的模板剂占总量的 93.0% 和 85.8%. 也就是说, 在相同初始凝胶摩尔比例的情况下, 几种模板剂用于平衡骨架电荷的用量比例顺序为 TEA > DEA > MOR.

表 7 不同模板剂合成的 SAPO-34 中骨架电荷数和最大 Si(4Al) 量

Table 7 Net charge of SAPO-34 samples synthesized using different templates and the maximum Si(4Al) contents

Sample	Net charge per mole (Al + Si + P)	A_1[a]	A_2[b]	Maximum Si(4Al) content[c]
T-0.6Si	–0.0897	1.07	0	0.068
DT-0.6Si	–0.1120	1.34	0	0.091
D-0.6Si	–0.1326	1.59	0.12	0.111
M-0.6Si	–0.1262	1.51	0.25	0.116
D-0.4Si	–0.1280	1.54	0.17	0.116

[a]Template number per cage used for balancing the net charge;
[b]Template number per cage – A_1;
[c]Maximum Si(4Al) content in SAPO-34 per mole (Al + Si + P).

根据各样品硅含量和 Si(4Al) 比例, 算得不同模板剂合成 SAPO-34 骨架中允许出现的最大 Si(4Al) 量, 即骨架中硅含量大于该值后, 其它硅环境开始出现, 结果列于表 7. DEA 和 MOR 合成的样品最大 Si(4Al) 量接近, 明显大于 TEA 合成的样品.

3 结论

以 DEA 为模板剂合成了 SAPO-34 分子筛, 并与其它模板剂进行了比较. 发现 DEA 导向合成 SAPO-34 的较佳条件为 $0.7 \le n(P_2O_5)/n(Al_2O_3) \le 1.2$ 和 $25 \le n(H_2O)/n(Al_2O_3) \le 100$. 铝源对所得 SAPO-34 样品组成的影响较大. 在 200 ºC 晶化 24 h 条件下, DEA 合成的样品结晶度和骨架硅含量最高, TEA 合成的样品最低, MOR 的介于中间. 这与模板剂促使硅进入骨架的能力顺序 DEA > MOR > TEA 有关. 以 DEA 和 MOR 为模板剂合成样品允许出现的最大 Si(4Al) 量接近, 明显大于 TEA 的. DEA-TEA 混合模板剂合成的样品则体现出两种模板剂的加和效应.

参 考 文 献

1 Qi G Z, Xie Z K, Yang W M, Zhong S Q, Liu H X, Zhang Ch F, Chen Q L. *Fuel Process Technol*, 2007, **88**: 437
2 Park Y K, Baek S W, Ihm S K. *J Ind Eng Chem*, 2001, **7**: 167
3 Hunger M, Seiler M, Buchholz A. *Catal Lett*, 2001, **74**: 61
4 Arstad B, Kolboe S. *Catal Lett*, 2001, **71**: 209
5 Liang J, Li H Y, Zhao S Q, Guo W G, Wang R H, Ying M L. *Appl Catal*, 1990, **64**: 31
6 Wilson S, Barger P. *Microporous Mesoporous Mater*, 1999, **29**: 117
7 Lok B M, Messina C A, Patton R L, Gajek R T, Cannan T R, Flanigen E M. US 4 440 871. 1984
8 Briend M, Vomscheid R, Peltre M J, Man P P, Barthomeuf D. *J Phys Chem*, 1995, **99**: 8270
9 Dumitriu E, Azzouz A, Hulea V, Lutic D, Kessler H. *Microporous Mater*, 1997, **10**: 1
10 Vistad Ø B, Akporiaye D E, Taulelle F, Lillerud K P. *Chem Mater*, 2003, **15**: 1639
11 Buchholz A, Wang W, Xu M, Arnold A, Hunger M. *Microporous Mesoporous Mater*, 2002, **56**: 267
12 Wei Y X, Zhang D Z, Xu L, Chang F X, He Y L, Meng S H, Su B L, Liu Z M. *Catal Today*, 2008, **131**: 262
13 刘中民, 蔡光宇, 何长青, 杨立新, 王作周, 罗静慎, 常彦君, 石仁敏, 姜增全, 孙承林 (Liu Zh M, Cai G Y, He Ch Q, Yang L X, Wang Z Zh, Luo J Sh, Chang Y J, Shi R M, Jiang Z Q, Sun Ch L). CN 1 088 483. 1994
14 何长青, 刘中民, 蔡光宇, 杨立新, 王作周, 罗静慎, 潘小珊, 盖增全, 常彦君, 石仁敏 (He Ch Q, Liu Zh M, Cai G Y, Yang L X, Wang Z Zh, Luo J Sh, Pan X Sh, Gai Z Q, Chang Y J, Shi R M). CN 1 096 496. 1994
15 Liu G Y, Tian P, Li J Z, Zhang D Z, Zhou F, Liu Z M. *Microporous Mesoporou Mater*, 2008, **111**: 143
16 Liu G Y, Tian P, Zhang Y, Li J Z, Xu L, Meng S H, Liu Z M. *Microporous Mesoporou Mater*, 2008, **114**: 416
17 Pastore H O, Coluccia S, Marchese L. *Ann Rev Mater Res*, 2005, **35**: 351
18 李军, 张凤美, 李黎声, 舒兴田. 石油炼制与化工 (Li J, Zhang F M, Li L Sh, Shu X T. *Petrol Process Petrochem*), 2005, **36**(6): 49
19 Lee Y J, Baek S C, Jun K W. *Appl Catal A*, 2007, **329**: 130
20 何长青, 刘中民, 杨立新, 蔡光宇. 催化学报 (He Ch Q, Liu Zh M, Yang L X, Cai G Y. *Chin J Catal*), 1995, **16**: 33
21 刘红星, 谢在库, 张成芳, 陈庆龄. 化学物理学报 (Liu H X, Xie Z K, Zhang Ch F, Chen Q L. *Chin J Chem Phys*), 2003, **16**: 521
22 Prakash A M, Unnikrishnan S. *J Chem Soc*, *Faraday Trans*, 1994, **90**: 229

英 译 文

English Text

Owing to their porous structure, moderate acidity, and good hydrothermal stability, SAPO-34 molecular sieves show a high selectivity towards light olefins in the methanol-to-olefin (MTO) reaction [1–6].

SAPO-34 can be synthesized using organic amines as templates, such as tetraethylammonium hydroxide [6–8], isopropylamine [7], dipropylamine [7], piperidine [9], morpholine (MOR) [7,10], triethylamine (TEA) [11–13], diethylamine (DEA) [14–16], and mixtures thereof. It is generally acknowledged that the template can play structure-directing, charge-compensating, and space-filling roles in the synthesis of molecular sieves [17]. The template exerts a significant influence on both the structures and properties

of the molecular sieves. A number of reports mainly focus on the effects of templates on crystal size and catalytic performance [18–21]. Investigations into the intrinsic reasons of how templates influence SAPO-34 acidity (i.e. how do the templates impact Si incorporation and distribution) are relatively scarce.

We have recently investigated the synthesis and catalytic properties of SAPO-34 in the MTO reaction, synthesized using DEA as a template [15]. In the present paper, we probe the influencing factors in the synthesis of SAPO-34, templated with DEA, to obtain the optimal synthesis conditions. Furthermore, a comparative study into several commonly used templates in the synthesis of SAPO-34, including DEA, TEA, and MOR, was performed to reveal the characteristics of samples prepared using different templates.

1 Experimental

1.1 Synthesis

SAPO-34 was synthesized using a hydrothermal method. The Si source (unless stated otherwise, it is silica sol), the Al source (unless stated otherwise, it is pseudoboehmite), phosphoric acid, and distilled water were mixed and stirred at room temperature. The template was added 1 h later and the resulting mixture was stirred until homogeneous. The gel was transferred to a 200 ml Teflon-lined stainless-steel autoclave, and heated and crystallized at 200 °C under autogenic pressure for 24 h. The typical molar composition of the gel was 2.0DEA:0.6SiO_2:1.0Al_2O_3:0.8P_2O_5:50H_2O. After crystallization, the as-synthesized sample was obtained after centrifugal separation, washing and drying in air at 120 °C. Calcination was then carried out in air at 550 °C for 5 h to remove the organic template.

1.2 Characterization

Powder XRD patterns were recorded on a Rigaku D/MAX-γB X-ray diffractometer using Cu K_α radiation (λ = 0.15406 nm) at 40 kV/40 mA. The crystal morphology was analyzed via scanning electron microscopy (SEM, KYKY-AMRAY-1000B). The chemical composition of the sample was obtained on a Philips Magix-2424 X-Ray Fluorescence (XRF) spectrometer.

Thermal analyses were measured on a Perkin Elmer Pyris-1 TGA analyzer, at a temperature-programmed rate of 10 °C/min under an air flow.

^{29}Si MAS NMR spectra were recorded in 7 mm ZrO_2 rotors at 79.5 MHz on a Varian Infinity-plus 400 WB spectrometer, fitted with a BBO probe. The spinning rate of the samples at the magic angle was 4 kHz. The internal standard for chemical shifts was 2,2-dimethyl-2-silapentane-5-sulfonate sodium salt (DSS).

2 Results and discussion

2.1 Influence factors in the synthesis of SAPO-34 templated by DEA

2.1.1 H_3PO_4 content

The effect of H_3PO_4 content (i.e. P_2O_5 content) on the synthesis was investigated with a gel molar composition of 2.0DEA:0.6SiO_2:1.0Al_2O_3:*n*P_2O_5:50H_2O. The XRD patterns for the obtained samples are shown in Fig. 1. With increasing P_2O_5 content, the pH values, before and after crystallization, obviously decrease and the products undergo a regular change. When n = 0.5, the product is obtained as an amorphous boehmite. When n = 0.6, SAPO-34 is formed. Pure SAPO-34 crystals can be obtained with $0.7 \le n(P_2O_5) \le 1.2$. SAPO-41, with an AFO structure and 10-ring channels, is formed with increasing n. When n = 1.5, no SAPO-34 is observed.

2.1.2 H_2O content

The influence of the H_2O level on the synthesis was investigated with gel molar compositions of 2.0DEA:0.6SiO_2:1.0Al_2O_3:0.8P_2O_5:*n*H_2O. XRD results show that SAPO-34 can be synthesized with $15 \le n(H_2O) \le 300$. Table 1 shows that the pH is almost consistent for all samples (about 6.0). After crystallization, the pH values decrease with increasing H_2O. The relative yields of SAPO-34 decrease with increasing H_2O content (i.e. $n \ge 25$). The relative crystallinity reaches its optimum value when n = 50. This rises with increasing $n(H_2O)$ when $n < 50$, but descends when $n > 50$. When n = 300, the relative crystallinity decreases to 33% and amorphous aluminum species begin to appear.

The chemical analysis given in Table 1 indicates that the silicon content in SAPO-34 declines with increasing H_2O content. A reduced H_2O content in the gel leads to a higher ion concentration, favoring synthesis. With the formation of products, the pH of the system rises. This increases the product solubility in the gel and reduces the yield. In a former study [15], the silicon content in the SAPO-34 increased with increasing DEA content (with increasing pH), whilst the crystal yield decreases. A larger H_2O content in the gel causes a lower ion concentration and a reduced driving force for synthesis. This results in a lower yield. Therefore, the optimal H_2O level ranges between $25 \le n(H_2O) \le 100$.

2.1.3 Si sources and Al sources

The influences of the Si (silica sol, fume silica and tetra-

ethoxysilane) and Al sources (pseudoboehmite, aluminum isopropoxide, aluminum chloride and alumina sol) on the synthesis were investigated with a gel molar composition of 2.0DEA:0.6SiO_2:1.0Al_2O_3:0.8P_2O_5:50H_2O. The results are shown in Table 2. Except for sample synthesized with alumina sol as the Al source and silica sol as the Si source, all compositions generated pure SAPO-34 with high crystallinity. The preparation of SAPO molecular sieves requires weakly acidic or neutral conditions. The pH value for the system with alumina sol as the Al source is too low (0.5), which leads to the formation of a quartz phase.

The chemical analysis given in Table 2 suggests that the Al source has a significant effect on the compositions of the as-synthesized samples. When silica sol is used as the Si source, sample using aluminum isopropoxide as the Al source, gives the lowest silicon content. Meanwhile, sample using pseudoboehmite as the Al source, gives the highest. This may be due to the higher reactivity of the monomeric Al source (aluminum isopropoxide) towards H_3PO_4, compared with the polymeric Al source (pseudoboehmite). An aluminophosphate precursor can form upon mixing aluminum isopropoxide with H_3PO_4. However, silica sol is a polymeric Si source, and the rate of depolymerization to give the active Si species is relatively slow. The Si substitution processes, for either P or P-Al pairs within the framework, were inhibited, which leads to the lower silicon content in sample. With pseudoboehmite as the Al source, the silicon contents for samples using fume silica and tetraethoxysilane as the Si source are the same. Both are slightly higher than that for sample using silica sol as the Si source.

Figure 2 presents the SEM images for the samples synthesized with the different Al and Si sources. The SAPO-34 crystals are rhombohedra. The crystal sizes in the samples synthesized with fume silica (a) and tetraethoxysilane (b) are clearly smaller than those obtained with silica sol (c, d, e) as the Si source.

2.2 Comparative study for SAPO-34 samples synthesized with different templates

The templates used in the comparative study include DEA, TEA, MOR, and a DEA-TEA mixture. The gel compositions and crystallization conditions are shown in Table 3.

2.2.1 Crystal phase and chemical composition

Figure 3 shows the XRD patterns for samples synthesized using the different templates. All XRD patterns are in agreement with those of SAPO-34 reported in the literature. With the exception of sample T-0.6Si (templated with TEA), all samples exhibit a relatively high crystallinity (see Table 4). The main peaks in the XRD for sample T-0.6Si are of high intensity, whilst the high-angle peaks are either weak or missing. This may be due to crystal structure distorting or the formation of eutectic SAPO-34 and SAPO-18 (trace amounts of SAPO-18).

Of the samples obtained with 0.6Si, that using DEA as the template, lead to the highest Si content (n(Si)/n(Si + Al + P) = 0.150). Meanwhile, that templated with TEA gave the lowest (n(Si)/n(Si + Al + P) = 0.102). This suggests that DEA templated SAPO-34 exhibits the appropriate characteristics for high silicon incorporation. The silicon content in sample DT-0.6Si, which was templated with a DEA-TEA mixture, is approximately equal to the average for samples D-0.6Si and T-0.6Si, consistent with the additive effect.

2.2.2 Crystal morphology

Figure 4 presents the SEM images for the samples synthesized with different templates. The crystal size for sample M-0.6Si, templated with MOR, is the largest (up to 10 μm), whilst that for sample T-0.6Si is the smallest (about 2 μm). The crystal size in sample D-0.6Si is in the range of 2–4 μm, which is slightly larger than that of T-0.6Si. The crystal size of DT-0.6Si is between those of samples D-0.6Si and T-0.6Si.

2.2.3 Thermal analysis

The TG profiles for the samples synthesized with the different templates reveal three stages of weight loss at < 200 °C, 200–490 °C, and > 490 °C, respectively. The first stage is attributed to water desorption from the sample. The second and third stages are due to the combustion decomposition of the template and the organic residues. The data given in Table 5 indicates that the weight losses associated with water desorption are close for all samples, while those due to the template vary significantly. The weight loss with TEA is the lowest (11.83%), whilst that with MOR is the highest (16.53%). The highest template mole number per cage, calculated based on the template weight loss, was found to be 1.76 for MOR, which is close to the result calculated by Prakash et al. [22]. The mole numbers obtained with TEA and DEA were found to be 1.02 and 1.71, respectively. The mole number for the DEA-TEA mixture was significantly higher than that obtained with TEA. The differences in the mole numbers per cage mainly come from the differences in molecular size. With three ethyl side chains, the molecular size of TEA is obviously larger than that of DEA, which only has two ethyl side chains.

In addition to the structure-directing and space-filling roles, the template also plays a charge-compensating role in the synthesis of molecular sieves. The positive charge provided by the template determines the negative charge of the framework. This arises from the Si substitution of the P or

P-Al pairs in framework. Therefore, the template mole number per cage influences the silicon content in framework to a certain degree. Since the TEA mole number per cage is the lowest, the associated silicon content in T-0.6Si is also lowest. Although the mole numbers for DEA and MOR per cage are similar, the silicon content in D-0.6Si is higher than that of M-0.6Si. Portions of the MOR in the cage may not play a charge-compensating role.

2.2.4 ^{29}Si MAS NMR analysis

The Si distribution in SAPO-34 framework can be characterized by ^{29}Si MAS NMR. Figure 5 shows the ^{29}Si MAS NMR spectra for the as-synthesized samples. Every sample presents a different Si distribution. According to the literature [11,17], the peaks at δ = –92.5, –96.5, –101, –105, and –111 are ascribed to Si(4Al), Si(3Al), Si(2Al), Si(1Al), and Si(0Al) environments, respectively.

Table 6 shows the distribution of the silicon environments, as evaluated from Gaussian fitting. Upon Comparing the D-0.4Si with D-0.6Si samples, the proportion of Si(4Al) environments decreases with increasing silicon content in the framework. Meanwhile, the proportions of the other Si environments increase. From the series of samples with 0.6Si, the proportion of Si(4Al) environments is at its lowest in sample T-0.6Si and at its highest in sample M-0.6Si. The distribution of silicon environments in sample M-0.6Si is similar to that in sample D-0.4Si. The distribution of silicon environments in sample DT-0.6Si is a cross between those for samples D-0.6Si and T-0.6Si.

The net charge in framework and the template number per cage (A_1) can be calculated based on the proportion of Si environments and the silicon contents in each sample (Table 4). In combination with the template mole number per cage in Table 5, the residual template number per cage (A_2), which is not used for balancing the net charge, can be obtained. The results are shown in Table 7. Upon comparing samples D-0.4Si and D-0.6Si, although their template numbers per cage are close, the template number used for balancing the net charge increases with increasing silicon content. The A_2 values for samples T-0.6Si and DT-0.6Si are both zero, which means all the templates in the cage are used to balance the framework charge. The A_2 values for samples D-0.6Si and M-0.6Si are 0.12 and 0.25, meaning the percentages of template used for balancing the framework charge are 93.0% and 85.8%, respectively. Hence, with the same initial gel, the percentage of template number used for balancing the framework charge follows the order TEA > DEA > MOR.

Based on the silicon content and Si(4Al) proportion for the various samples, the maximum Si(4Al) content within the SAPO-34 can be obtained. Other Si environments will appear when the silicon content increases beyond the maximum Si(4Al) level. This indicates that the maximum Si(4Al) contents for samples D-0.6Si and M-0.6Si are similar, and significantly greater than that of T-0.6Si.

3 Conclusions

In the present paper we have investigated the synthesis of SAPO-34 molecular sieves templated with DEA, and compared their properties with those synthesized using different templates. The optimal synthesis conditions for the DEA templated SAPO-34 are $0.7 \leq n(P_2O_5)/n(Al_2O_3) \leq 1.2$ and $25 \leq n(H_2O/Al_2O_3) \leq 100$. The Al source has a great influence on the resulting sample composition. A comparative study revealed the DEA templated sample to have the highest crystallinity and silicon content. MOR had the second highest, and TEA the lowest. This is related to the templates ability to promote Si incorporation into the SAPO-34 framework, which follows the order DEA > MOR > TEA. The maximum Si(4Al) contents for samples templated with DEA and MOR are similar, but both were significantly greater than that observed with TEA. The properties for the samples templated with a DEA-TEA mixture are consistent with the additive effect.

Full-text paper available online at Elsevier ScienceDirect
http://www.sciencedirect.com/science/journal/18722067